



Contents lists available at ScienceDirect

Catalysis Today

journal homepage: www.elsevier.com/locate/cattod



Versatile heterogeneous dipicolinate complexes grafted into kaolinite: Catalytic oxidation of hydrocarbons and degradation of dyes

Francielle R. Araújo^a, Joel G. Baptista^a, Liziane Marçal^a, Katia J. Ciuffi^a, Eduardo J. Nassar^a, Paulo S. Calefi^a, Miguel A. Vicente^b, Raquel Trujillano^b, Vicente Rives^b, Antonio Gil^c, Sophia Korili^c, Emerson H. de Faria^{a,*}

^a Sol-Gel Group, University of Franca, Av. Dr. Armando Salles Oliveira, Parque Universitário, 201, 14404-600, Franca, SP, Brazil

^b GIR QUESCAT, Departamento de Química Inorgánica, Universidad de Salamanca, Plaza de la Merced, S/N, 37008 Salamanca, Spain

^c Departamento de Química Aplicada, Universidad Pública de Navarra, 31006 Pamplona, Spain

ARTICLE INFO

Article history:

Received 25 June 2013

Received in revised form

15 September 2013

Accepted 23 September 2013

Available online xxx

Keywords:

Kaolinite

Heterogeneous catalysis

Dipicolinate complexes

Oxidation reactions

Dyes degradation

ABSTRACT

New heterogeneous catalysts were prepared by immobilization of Me(II)-dipicolinate complexes (Me = Co, Mn or Ni) on kaolinite (Ka). The precursor material was kaolinite grafted with dipicolinic acid (dpa) obtained via melting of the acid. The catalysts were prepared by suspending the Ka-dpa precursors (lamellar or exfoliated) in Me²⁺ solutions with a cation/ligand ratio of 1:3. The grafted complexes were characterized by thermal analyses, X-ray diffraction, UV/Vis and infrared spectroscopies, and transmission electron microscopy. The catalysts were tested in three reactions: (i) epoxidation of *cis*-cyclooctene to *cis*-cyclooctenoxide reaching 55% yield, with total selectivity to cyclooctenoxide; (ii) oxidation of cyclohexane, reaching 22% yield, with total selectivity towards cyclohexanone; and (iii) Fenton-like decolorization of the dyes metanil yellow, methylene blue and green light, reaching 70–100% decolorization, the maximum effectiveness being observed for methylene blue degradation. The high conversion in the oxidation reactions and the high levels of decolorization of dyes confirmed the versatility of these heterogeneous catalysts based on kaolinite.

© 2013 Elsevier B.V. All rights reserved.

1. Introduction

The need to develop effective methods and catalysts for oxidation reactions is becoming ever more important to be commonly applied to synthesis of pharmaceuticals, agrochemicals, and flavours or fragrances, among others. From an industrial point of view, homogeneous catalysis methods remain unpractical, particularly due to the high cost of the catalysts and the difficulty of their recovery and reuse [1]. Thus, from an economic, environmental and technical point of view, heterogeneous supported catalysis is preferred because of the handling, separation and recycling abilities. The functionalization of clay minerals, such as kaolinite, with organic units renders the possibility of heterogeneization of active sites and promotes the reuse. Recently, our research group has reported the functionalization of natural kaolinite with pyridine-carboxylic acids, alkoxides, and ironporphyrins by the soft-guest displacement method [2,3].

In recent years, much interest has been given to hybrid materials based on clays. These materials are produced by several reactions and can lead to intercalation compounds with various applications, depending on the type of interaction between the inorganic matrix and the intercalated species. Transition metal complexes show high catalytic activity and selectivity in hydrocarbon oxidations in homogeneous media, but they have high difficulty to be recovered and reused. An alternative for applications requiring high temperature during the process, and more catalytic cycles with high conversion and selectivity, is based on the use of these complexes immobilized on/into inorganic matrices. A “heterogeneization” is made in this method, as the complexes are immobilized in inorganic matrices such as kaolinite, able to modify the kinetics and mechanism of the reactions. Hybrid materials have been explored for this purpose and, among them, the kaolinite-based materials stand out due to the high thermal stability of the hybrids obtained.

The search for efficient and environmentally friendly oxidation systems that could be used in green processes for several oxidation reactions has been recently intensified [4,5]. Transition metals are used in a large variety of catalytic processes. Bergamaschi et al. [6] used transition metals supported on zirconia in reactions of steam reforming of ethanol to obtain hydrogen. Thomas et al. [7]

* Corresponding author.

E-mail address: eh.defaria@unifran.br (E.H. de Faria).

reported the use of manganese and cobalt catalysts in the oxidation of toluene by hydrogen peroxide. Sen et al. [8] and Gupta et al. [9] demonstrated the effectiveness of nickel and manganese heterogeneous catalysts in oxidation reactions. Previous studies from our group [2,10] have demonstrated the efficient use of kaolinite as a support for metalloporphyrin and iron(III)-picolinate and dipicolinate complexes to obtain catalytic systems with good performance and high selectivity in *cis*-cyclooctene, cyclohexane and Baeyer-Villiger oxidation.

The transfer of oxygen atoms to carbon substrates, to understand or to mimic enzymatic porphyrin systems, has been previously reported [11], as well as the study of non-heme enzymatic model systems, such as metal complexes, to catalyze these reactions. In particular, Schiff base complexes are potentially applicable as catalysts in several oxidation reactions, including alkene epoxidation and hydrocarbon oxidation [9,12].

Industrial processes normally involve oxidation reactions in the presence of a metal complex as a catalyst, together with acids and permanganate as oxidant, in an homogeneous medium. However, these processes involve serious problems, namely, difficulty to recover the catalyst from the reaction medium, corrosion, and the need for expensive, hazardous, non-selective oxidants [9,12]. One strategy to overcome these drawbacks, is to heterogenize the metal complex by immobilizing it on a polymer or an inorganic matrix and to accomplish the reaction using cleaner oxidants like hydrogen peroxide or molecular oxygen, which generates water as the only byproduct. However, many efforts are still necessary to develop heterogeneous catalysts that do not undergo deactivation during the catalytic process [9,12,13].

About 15% of the total world production of dyes is lost during the dyeing process and is released to the textile effluents, and this release of these colored waste waters in the ecosystem is a dramatic source of non-aesthetic pollution, eutrophication and perturbations in the aquatic life [14]. As international environmental standards are becoming more severe, new methods for the removal of organic pollutants, such as industrial dyes, have been very much studied by various groups. Among them, physical methods (as adsorption) [15], biological methods (as biodegradation) [16], and chemical methods (as chlorination or ozonation) [17], are the most frequently used ones. In this context, many studies have demonstrated the applicability of heterogeneous catalytic technologies in “Fenton-like” systems, advanced oxidation processes that use hydrogen peroxide (H_2O_2) and metallic species for the treatment of hazardous organic and inorganic pollutants existing in aqueous media. The Fenton-type processes are very promising since they are easy to operate and maintain, they offer a cost effective source of hydroxyl radicals, and achieve high conversions. The conventional production of HO^\bullet radicals by the Fenton mechanism occurs by means of addition of H_2O_2 to Fe^{2+} according to the reaction: $Fe^{2+} + H_2O_2 \rightarrow Fe^{3+} + HO^\bullet + HO^-$ [18]. Recently, some other metals have been used to generate HO^\bullet radicals [19,20].

On the other hand, dyes have been extensively used as model compounds for the evaluation of new catalysts, among other factors by the simplicity for following their reactions, especially decolorization. New research in the preparation of innovative Fenton-like reactions has been motivated by two main issues, namely, the improvement of the efficiency in the use of green oxidants, and the immobilization of the active sites into inert supports to facilitate the separation of the catalysts when the reaction has finished.

This work reports the catalytic study of Me(II)-dipicolinate complexes (Me = Co, Mn or Ni) immobilized into kaolinite. The grafted complexes were used as heterogeneous environmental-friendly catalysts in the epoxidation of *cis*-cyclooctene to cyclooctenoxide,

in the oxidation of cyclohexane to cyclohexanol and cyclohexanone, and in the degradation of three dyes (metanil yellow, methylene blue and green light).

2. Experimental

2.1. Catalyst preparation

2.1.1. São Simão' kaolinite purification

The kaolinite used in this work came from the municipality of São Simão in the State of São Paulo, Brazil, and was kindly supplied by the mining company Darcy R. O. Silva & Cia. It belongs to the ball-clay type, known for its fine granulometry and for being rich in hexagonal kaolinite. Kaolinite was purified by dispersion in water, followed by sedimentation, according to Stock's law and using the procedure previously described [4,21–23]. The structural formula of purified kaolinite is $Si_2.0Al_{1.96}Fe_{0.03}Mg_{0.01}K_{0.02}Ti_{0.03}O_{7.06}$ [3].

2.1.2. Kaolinite intercalation with dimethylsulfoxide

To obtain the precursor intercalated with dimethylsulfoxide (Ka-DMSO), the method described by Detellier et al. was followed [8,9]. A portion of 20 g of the purified kaolinite was suspended in a mixture of 180 cm³ of DMSO and 20 cm³ of H₂O, which was maintained at 60 °C under agitation for 10 days. The material was centrifuged at 2000 rpm, washed with ethanol and oven-dried at 60 °C. The resulting complex, designated as Ka-DMSO, has the stoichiometry $Ka(DMSO)_{0.45}$.

2.1.3. Kaolinite grafting with dipicolinic acid

The hybrid organic-inorganic material was obtained by keeping a mass of the precursor (Ka-DMSO) in the presence of the melted dipicolinic acid for 48 h. The dipicolinic acid/kaolinite DMSO complex molar ratio was 5:1. The temperature for grafting H₂dpa acid was 190 °C. The resulting materials were washed several times with isopropanol or water and oven-dried at 80 °C. The first sample was washed several times with isopropanol, the second washed with water, and the third with isopropanol and suspended in an ultrasonic bath for 8 h to promote the exfoliation of the hybrid precursor; finally, all these samples were oven-dried at 80 °C and designated as Ka-dpa-IP, Ka-dpa-wt and Ka-dpa-exf, respectively.

2.1.4. Synthesis of the complexes immobilized into kaolinite

To obtain the metal-containing catalysts, Ka-dpa solids were suspended in a 0.1 mol/dm³ Me²⁺ chloride solution (Me²⁺ = Co²⁺, Mn²⁺ and Ni²⁺), using the volume needed to reach a cation/ligand ratio of 1:2, and the mixture was stirred at 80 °C for 3 h. The suspensions were then centrifuged, and the resulting solids were washed with ethanol five times. The catalysts obtained were designated as Me(Ka-dpa)-IP, Me(Ka-dpa)-wt and Me(Ka-dpa)-exf, making reference to the active metal and the method of preparation of the hybrid precursor.

2.2. Characterization techniques

The powder X-ray diffractograms of the solids were acquired on a Siemens D-500 diffractometer operating at 40 kV and 30 mA (1200 W), using filtered Cu K α radiation. All the analyses were processed at a scan speed of 2° per minute.

Infrared absorption spectra were obtained on a Perkin-Elmer 1739 spectrophotometer with Fourier transform, using the KBr pellet technique.

UV-Vis spectra were recorded in the 200–800 nm range on a HP 8453 Diode Array Spectrophotometer. The spectra of the solid samples were recorded in a quartz cell with 0.1 cm path length, in ethanol suspension.

Thermal analyses were carried out in a TA Instruments SDT Q600 Simultaneous DTA-TGA thermal analyzer, in the temperature range between 25 and 1100 °C, at a heating rate of 10 °C/min and air flow of 100 cm³/min.

Transmission electron microscopy (TEM) was performed using a Zeiss-902 microscope over samples ground and dispersed in ethanol by using an ultrasonic apparatus; then, a drop of the suspension was placed on a Cu grid and air dried before the study.

2.3. Catalytic performance

2.3.1. Oxidation of *cis*-cyclooctene and cyclohexane

Catalytic oxidation reactions were carried out at 25 °C in a 2.0 cm³ glass reactor, sealed with a Teflon-coated silicone septum and equipped with a magnetic stirrer. When the oxidant was hydrogen peroxide, the Me-(Ka-dpa) catalyst was suspended in 1 cm³ of the solvent mixture (1,2-dichloroethane/acetonitrile, 1:1, v/v), and the substrate was added, resulting in a constant catalyst/oxidant/substrate molar ratio of 1:300:100.

When the oxidant was iodosylbenzene (PhIO), it was first obtained through hydrolysis of iodosylbenzene diacetate [24], and its purity was evaluated by iodometric titration [25]. PhIO (0.023 mmol) was added to the reactor containing the catalyst (10 mg) and the dichloroethane/acetonitrile solvent mixture (1 cm³). Then, 1.15 mmol of the substrate (*cis*-cyclooctene or cyclohexane) and 10⁻² cm³ of di-*n*-butyl ether as internal standard were added.

The evolution of the reactions was followed by analyzing the products at fixed times of 2, 4, 24, or 48 h. The products were identified using a HP 6890 Series GC System gas chromatograph (with a flame ionization detector) equipped with a HP-INNOWax-19091N-133 (polyethylene glycol length 30 m, internal diameter 0.25 μm) capillary column. The products were quantified using a calibration curve obtained with a standard solution. When the oxidant was hydrogen peroxide, the conversion was based on the substrate, while when the oxidant was iodosylbenzene, the yield was based on the oxidant.

At the end of the reactions, the catalysts were recovered by centrifugation, dried for 3 h at 60 °C before being used again in a further catalytic cycle. The supernatant liquids were maintained in the reactor for 24 h, aftermost the possible products formed were quantified by GC. This simple test gave evidences of the leaching of active Me(II)-species from the solid to the liquid.

All solvents and reagents were purchased from Mallinckrodt, Aldrich, or Acros Organics and were of commercial grade, unless otherwise stated. Dichloromethane (DCM) was suspended on anhydrous CaCl₂ for 2.5 h, filtered, distilled over P₂O₅, and kept over 4 Å molecular sieves. *cis*-Cyclooctene, cyclohexane, cyclohexanol, and cyclohexanone were purified on a basic alumina column immediately before use. Hydrogen peroxide (solution in water) was donated by Peróxidos do Brasil and was iodometrically titrated before use.

2.3.2. Degradation of dyes in Fenton-like heterogeneous catalysis

The degradation of the dyes-metanyl yellow (MY, anionic), green light (GL, anionic) and methylene blue (MB, cationic) was tested in heterogeneous "Fenton-like" systems, using 10 mg of each Me(Ka-dpa) catalyst, 5 cm³ of 25 mg/dm³ dye solutions, and 0.1 cm³ of hydrogen peroxide (50% v/v), under a constant catalyst:dye:H₂O₂ mole ratio of 1:300:2000. The kinetics of dyes degradation was accomplished between 1 and 1740 min. The dye degradation and final concentration of each solution was quantified by the calibration curve accomplished in solution by UV-Vis spectroscopy using the characteristic band of each dye (MB: 665 nm, MY: 475 nm, GL: 625 nm).

3. Results and discussion

3.1. Characterization of the catalysts

The first steps of the synthesis procedure (purification of kaolinite, swelling with dimethylsulfoxide) are common for all samples, and have been previously reported [4]. The samples will be described in two series, in one of them the solids washed with water or isopropanol after treatment with dipicolinic acid, and in a second series the solids submitted to ultrasonic exfoliation.

3.1.1. Kaolinite-dipicolinate hybrid systems washed with water or isopropanol

The X-ray diffractograms of the catalysts derived from kaolinite are shown in the Supplementary Material (Fig. S1). The solids grafted with dipicolinic acid displayed basal spacings of 12.00 Å when washed with isopropanol and 11.75 Å when washed with water, characteristic values of kaolinite expanded with dpa [3]. The sample washed with water was much less ordered than that washed with isopropanol and it showed a clear peak at about 7.20 Å, corresponding to non-expanded layers, effect that is almost negligible in the sample washed with isopropanol.

Washing of grafted samples with isopropanol promoted the rearrangement of kaolinite layers, while washing with water promoted the disorder of kaolinite layers [4]. The hydrogen bonds between the aluminol (Al-OH) and siloxane groups (Si-O) in kaolinite were weakened in grafted samples, and further washing with high polar solvents such as water promoted the structural disorder by repulsion of the aluminol grafted to the dpa hydrophobic surface and attracted by the siloxane surface.

The reaction ratio was quantified, and the percentage of layers intercalated decreased from 90% in Ka-dpa-IP to 59% in Ka-dpa-wt. This suggests that washing with small and strongly polar molecules promotes the partial lixiviation of the intercalated ligands. The intercalation ratio was calculated on the basis of the relative intensities of the 001 peak, characteristic of stacking of the layers in the *c*-direction, so the low value found for the sample washed with water is justified by the strong affinity of the siloxane layer to water molecules, that promotes the structural disorder (see Table S1).

The infrared spectra of Ka, Ka-DMSO, Ka-dpa-IP and Ka-dpa-wt displayed bands at 3699 and 3618 cm⁻¹, characteristic of inner- and inner surface hydroxyls, respectively (Fig. S2 and Table S2). The other bands for inner surface hydroxyls existing in kaolinite and in the kaolinite-DMSO sample were weakened (at 3653 cm⁻¹) or even were not observed (3668 cm⁻¹), thereby confirming the functionalization of the kaolinite matrix. A new band at 3600 cm⁻¹ was assigned to the formation of hydrogen bonds between the unreacted inner-surface hydroxyl groups of kaolinite with the carboxylate groups of the dpa molecules. It is also possible that a low amount of intercalated dpa molecules (in sample Ka-dpa-IP) are located in the interlayer space of kaolinite, since it might not have been totally removed, despite the exhaustive washing process. This band at 3600 cm⁻¹ was formerly observed upon grafting and/or intercalation of molecules such as polyols, ethylpyridinium, and D-sorbitol into kaolinite [26–28]. The diffusion of these intercalated molecules depends on the interactions between the grafted molecules and unreacted hydroxyl groups, which would contribute to the formation of the new band at 3600 cm⁻¹.

Bands characteristic of antisymmetric and symmetric stretching modes of the carboxylate group were observed at 1689, 1566 and 1478 cm⁻¹. The shift of the bands corresponding to inner surface hydroxyls and the development of new bands in regions related to the pyridine-carboxylic groups gave evidence of the grafting of dipicolinic acid molecules into the interlayer space of kaolinite. At the same time, the absence of C–H and S=O vibrations in the spectra showed the total substitution of DMSO molecules by the

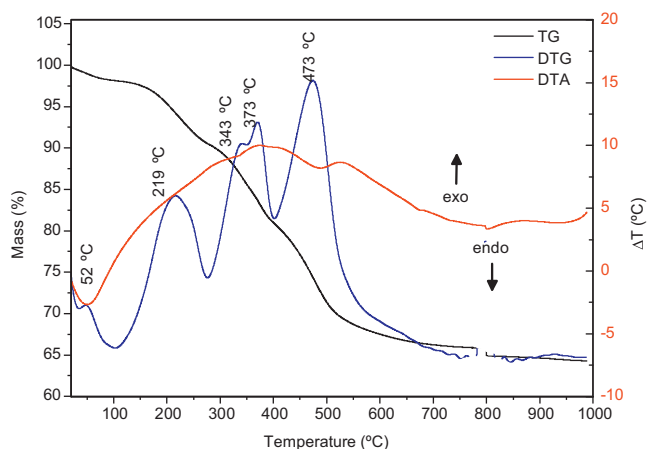


Fig. 1. TG, DTG and DTA curves of Ka-dpa-IP recorded in O₂ atmosphere.

dipicolinic acid [26–28]. In the specific case of the Ka-dpa-wt sample, characteristic antisymmetric and symmetric stretching mode bands from the carboxylate groups evidenced the functionalization of the kaolinite. The appearance of two bands (1695 and 1354 cm⁻¹) in the spectrum of the solid washed with water suggests that some carboxylate groups, possibly free or weakly bound to the clay structure, were interacting with water or hydroxyl groups existing in the interlayer space of kaolinite. At the same time, the characteristic vibration of the inner surface aluminol group (938 cm⁻¹) was absent, this being a further evidence that kaolinite was indeed functionalized, via covalent Al–O–C bonds between the clay and the dipicolinic acid [26–28].

The thermal behavior of kaolinite and the kaolinite–DMSO precursor has been previously reported [8,16,21,23–27]. The TG, DTG and DTA curves for grafted derivatives Ka-dpa-IP and Ka-dpa-wt are shown in Fig. 1 and S3 and the data summarized in Table S3. The TG curve for sample Ka-dpa-IP showed five mass loss stages; the first one with an endothermic peak at 52 °C (1.9%) was assigned to the elimination of the solvent used to wash the hybrid material. The second stage, with the maximum mass loss at 219 °C (7.7%), was assigned to removal of residual DMSO and/or acid intercalated into the kaolinite interlayer space. The third and fourth stages, centered at 343 °C (5.4%) and 373 °C (4.1%), were assigned to the decomposition of dpa molecules grafted into kaolinite. And the last mass loss (473 °C, 16.6%) was assigned to dehydroxylation of kaolinite and elimination of residual carbon from the interlayer space of kaolinite. These results were similar to those reported by de Faria et al. [10].

However, the TG curve for sample Ka-dpa-wt showed four mass loss stages. The first stage, with an endothermic peak at 64 °C (1.4%), was assigned to the removal of adsorbed water used to

wash the hybrid material. The second mass loss stage (235 °C, 3.8%) was assigned to removal of residual DMSO and/or dipicolinic acid intercalated into kaolinite, and the third stage (345 °C, 7.4%) was assigned to the decomposition of dpa grafted in the interlayer space of kaolinite. The appearance of a single stage mass loss in this region can be attributed to the removal of intercalated acid moieties during the washing process, so, the mass loss corresponding to grafted dpa decreased from 9.5% (Ka-dpa-IP) to 7.4% (Ka-dpa-wt). The fourth mass loss stage (487 °C, 15.2%) was attributed to the dehydroxylation of kaolinite and the decomposition of residual carbon from the interlayer space of kaolinite. Another effect noted is the variation in the temperature of kaolinite dehydroxylation, which decreases to 473 °C in Ka-dpa-IP and 487 °C in Ka-dpa-wt, respectively (513 °C in pure kaolinite). This decrease suggested a covalent bond between organic and inorganic units, by reaction with the aluminol surface of kaolinite [23,25,29–33].

Based on the thermal and chemical analysis results, the ratio of dpa molecules per unit cell of kaolinite was quantified, the resulting formulae being Ka(dpa)_{0.684} for sample Ka-dpa-IP and Ka(dpa)_{0.430} for sample Ka-dpa-wt. The C/N ratios in the functionalized solids were very close to that in the pure dpa molecule.

Fig. 2 shows that the basal reflection of intercalated kaolinite disappeared after complexation with the metallic cations. This happened in all solids, together with an increase in the intensity of the peak of non-expanded kaolinite, which suggests a different planar arrangement of kaolinite layers and dpa molecules when complexing the Me(II) ions. This rearrangement led to the formation of a crystalline phase with peaks at 8.39, 6.28, 5.95 and 5.48 Å, compatible with pseudo-tubular halloysite [34]. The structural change of kaolinite leading to the formation of nanotubes has been reported by Matusik et al. [35–37]. Halloysite is a clay mineral with a chemical formula very similar to that of kaolinite, and naturally occurs in a tubular form [37–39]. Formation of the tubular phase in kaolinite functionalized with dipicolinate complexed with Me(II) cations can be justified by the interaction between the Me(II)–dipicolinate complex and the inorganic matrix, thereby reducing the interactions between the layers and promoting their curling [40–43]. After immobilization of Me²⁺ species into the Ka-dpa precursor another fact that can contribute to the exfoliation process is the possible leaching of intercalated moieties of H₂dpa via a deintercalation process promoting the decrease of the basal spacing. However, the grafted species is very stable and remained grafted after insertion of cationic species into the interlayer space and remained intact in the exfoliated moieties. The XRD patterns revealed that the characteristic peak of non-expanded kaolinite at 7.14 Å, that remained with a small intensity in Ka-DMSO and Ka-dpa precursors, becomes broad after Me(II) incorporation, because of the presence of water molecules coordinated to the Me(II) complexes located in the interlayer of kaolinite.

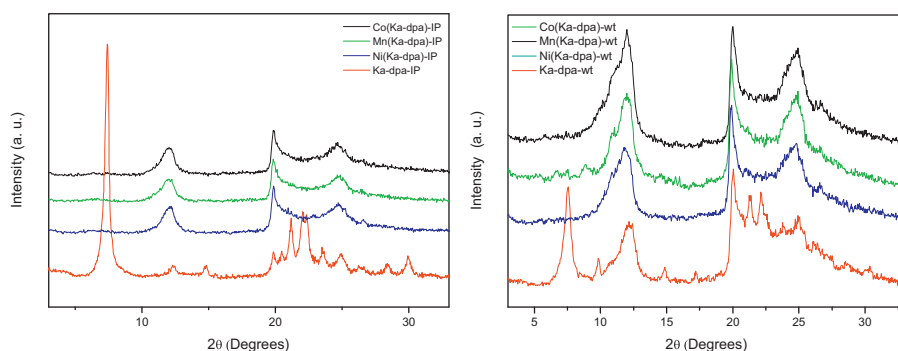


Fig. 2. X-ray powder diffraction patterns of the precursor Ka-dpa-IP (left) and Ka-dpa-wt (right), and heterogeneous catalysts obtained after complexation with Me(II) cations in aqueous media.

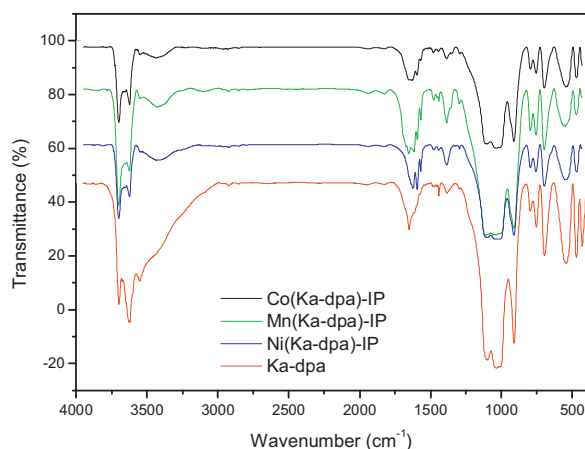


Fig. 3. Infrared spectra of the Ka-dpa-IP precursor and heterogeneous catalysts Me(Ka-dpa)-IP.

The infrared absorption spectra of the metal-containing catalysts, and the spectra of the precursors, are shown in Figs. 3 and S4, and the data summarized in Table S4. The vibrations of inner and inner surface hydroxyls of kaolinite at 3622 and 3698 cm^{-1} , respectively [3,29,30,32], are not shifted after complexation with Ni^{2+} , Mn^{2+} or Co^{2+} , showing that complexation did not promote the leaching of the ligands functionalized to aluminol groups of kaolinite [2,10]. The characteristic bands of grafted dipicolinate, due to the carboxylate group and the pyridine ring, were recorded in the central region of the spectrum, appearing at 1695, 1674, 1597, 1572, 1485, 1387 and 1354 cm^{-1} in the precursors, and shifting to 1651, 1599, 1572 and 1385 cm^{-1} after complexation with Ni^{2+} ; to 1654, 1597, 1572, 1481 and 1381 cm^{-1} in the case of Mn^{2+} and to 1653, 1595, 1570, 1481 and 1385 cm^{-1} for Co^{2+} , confirming the coordination of the cations to the carboxylate groups and the pyridine ring [3]. Álvaro et al. [44] have reported the incorporation of Fe(III) picolinate into zeolite Y and Na-mordenite, taking the band at 1480 cm^{-1} as a spectroscopic evidence of the formation of the Fe(pa)₃ complex. Gardolinski et al. [45] observed the development of a weak band at 3545 cm^{-1} upon treating kaolinite in aqueous solution, this band being attributed to the presence of water molecules in the interlayer region of kaolinite, interacting with the internal and external hydroxyls via hydrogen bonds. This band was evident in the spectra of all our solids, both when washed with water or with isopropanol.

The thermal behavior of some of the samples was investigated under oxygen atmosphere; the curves from Ni(Ka-dpa)-IP are given, as a representative example, in Fig. 4, while other curves and a summary of the thermal effects are included in the Supplementary Material (Fig. S5 and Table S5). The TG curves showed three mass losses, the first stage, centered at 60–70 °C, was assigned to removal of small amounts of solvent remaining in the solids. The second mass loss, centered at 355–390 °C, was assigned to the decomposition of the complex in the interlayer space of the clay, with the subsequent decomposition and elimination of dipicolinate ligands. The third stage, centered at 481–496 °C, corresponded to kaolinite dehydroxylation, and the elimination of residual carbon in the interlayer space of the kaolinite remaining from the previous process. Removal of residual carbon at these temperatures has been previously shown in kaolinite hybrids by Faria et al. [10] and Detellier and Tunney [22].

Fig. 5 and Fig. S6 show the UV-Vis spectra of solids Me(Ka-dpa), compared to the solution spectra of the Me(II) chlorides, the dpa ligand, and the compound Ka-dpa. The UV-Vis spectra of Ka-dpa displayed absorption bands at 204, 220, and 260 nm, characteristic of the absorption of dipicolinate grafted to kaolinite. For the

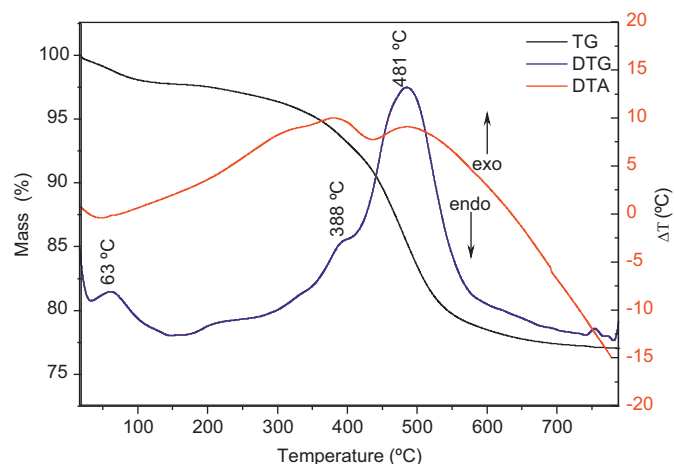


Fig. 4. TG, DTG and DTA curves of Ni(Ka-dpa)-IP carried out in O₂ atmosphere.

Me-containing solids, the bands at 196, 220, and 265 nm were associated to ligand to metal charge-transfer (LMCT) processes. These bands could reasonably be attributed to the complexation of Me(II) species with the dipicolinate units grafted on kaolinite [46]. However, other authors have considered that these bands were due to the d-d transfer to ²E_g state [47]. In our solids, this LMCT band might be due to an electron transfer from the nitrogen atoms or carboxylate groups of dpa anions grafted into kaolinite to the empty Me(II) orbitals. Another evidence of formation of typical Mn(II)-dpa complexes is observed in the visible region; the characteristic broad band with maximum at 430 nm, recorded after complexation, confirming the complexation of Mn(II) ions into the Ka-dpa hybrid matrix. Similar results were observed for the solids containing Ni(II) and Co(II).

3.1.2. Kaolinite-dipicolinate hybrid systems exfoliated via ultrasounds

Fig. 6 shows the powder XRD diffractograms of kaolinite functionalized with dipicolinic acid after submission to exfoliation treatments for 1–8 h in an ultrasound bath, compared to the original hybrid material Ka-dpa-IP. A structural rearrangement of kaolinite after the exfoliation treatment was observed, leading to the formation of the crystalline phase above described, similar to halloysite with a pseudo-tubular nature. This rearrangement was even evident from short times and complete for the longest times considered.

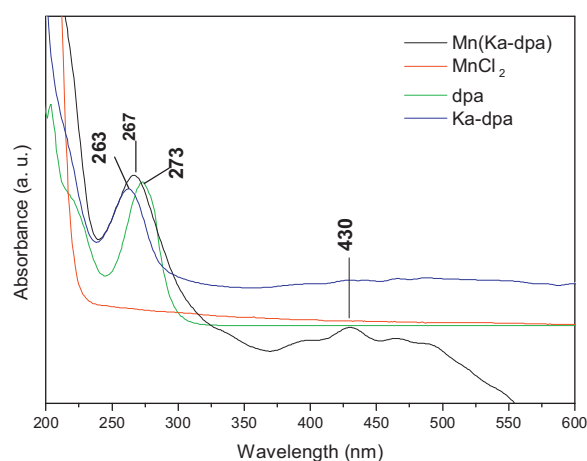


Fig. 5. UV-Vis spectra of Mn²⁺ chloride, dipicolinic acid (H₂dpa), Ka-dpa-IP, and catalyst Mn(Ka-dpa)-IP.

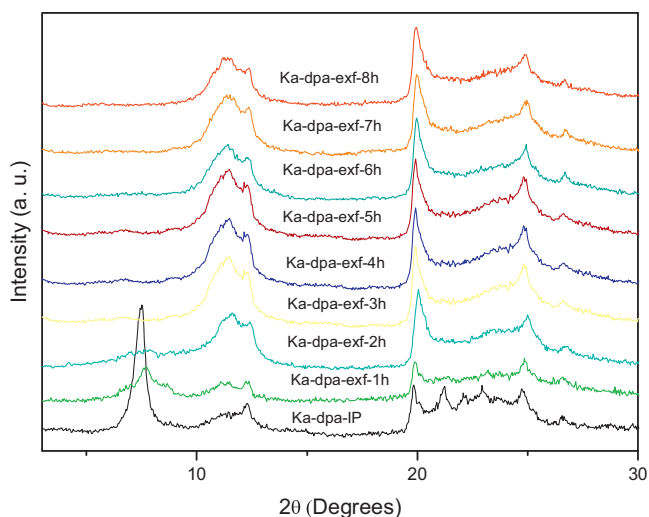


Fig. 6. X-ray powder diffraction patterns (detailed onset of the $2\theta = 5\text{--}30^\circ$ region) of the exfoliated solids compared to the precursor Ka-dpa-IP.

The infrared spectrum of the hybrid material exfoliated for 8 h with an ultrasonic bath and the precursor material (Ka-dpa-IP) is shown in Fig. S7. The exfoliated solid showed characteristic vibrations at 3699 ($\nu\text{OH}_{\text{inner surface}}$) and 3622 cm^{-1} ($\nu\text{OH}_{\text{inner}}$) [3,29,30,32]. Characteristic vibrations of the carboxylate groups appeared at 1647 and 1383 cm^{-1} , corresponding to the antisymmetric and symmetric stretching modes of these groups, indicating that the hybrid material kept grafted after the exfoliation process, what is confirmed by the absence of the characteristic vibration of the aluminol group from the inner surface (938 cm^{-1}). The decrease in the intensity of the characteristic C–H bands confirmed the presence of less dpa molecules in comparison to the precursor material Ka-dpa-IP.

Fig. S8 shows the thermal curves of the exfoliated hybrid material (Ka-dpa-xf). The mass loss stages between $60\text{--}405^\circ\text{C}$, characteristic of the decomposition of functionalized dpa, disappeared. The increased thermal stability of the hybrid may have been promoted by the folding of the structure of kaolinite, which led dpa molecules to be encapsulated within the pseudo-tubular structure [2,3,40]. The number of dpa molecules per unit cell of kaolinite was calculated based on thermal analysis, leading to the formula $\text{Ka}(\text{dpa})_{0.16}$, clearly showing the leaching of intercalated dpa units promoted by ultrasonics. That is, the number of dpa molecules is much lower, but these molecules are strongly grafted into the kaolinite tubular structure.

Complexation of $\text{Me}(\text{II})$ cations of the exfoliated precursor did not promote structural changes in the pseudo-halloysite like structure, all the XRD peaks remained in the same positions and with similar intensities for all metals (Fig. S9); the precursor Ka-dpa showed a basal spacing of 7.81 Å, but 7.70 , 7.59 and 7.59 Å after the complexation with Co^{2+} , Mn^{2+} , and Ni^{2+} , respectively. Grafting followed by exfoliation into kaolinite-dipicolinate layers difficult the formation of the pseudo-tubular phases.

After complexation with the divalent cations, the characteristic infrared bands of intra and interlayer hydroxyls and aluminol groups in kaolinite did not shift (Fig. S10), so the ligands continued covalently bonded to aluminol groups in the surface of kaolinite [10].

Thermogravimetric analysis of the catalysts based on Ka-dpa-xf (the curve for Mn-solid is given as an example in Fig. 7; those for the Ni- and Co-solids are included in Fig. S11) exhibited two mass loss stages, the first, endothermic one centered at $45\text{--}55^\circ\text{C}$, due to removal of small amounts of solvent remaining from the synthesis.

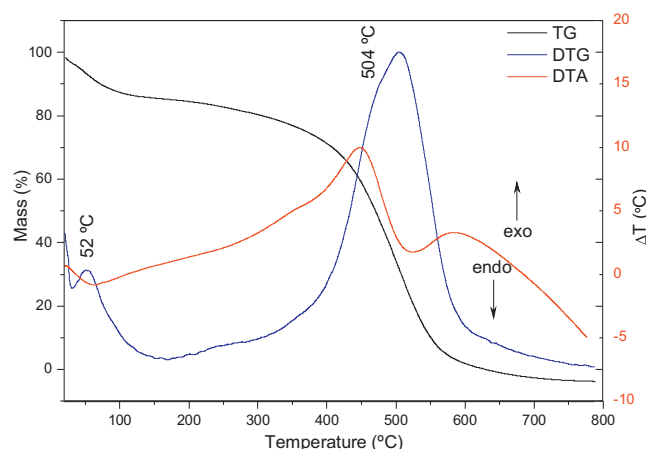


Fig. 7. Thermal curves of Mn(Ka-dpa)-xf carried out in O_2 atmosphere.

The second mass loss, exothermic, was centered close to 500°C , and assigned to the decomposition of the complexes and to the dehydroxylation of the pseudo-halloysite structure (the endothermic character of this process is masked by the decomposition of the ligands). As in the precursor, the decomposition of the clay occurs at a higher temperature when it has the pseudo-tubular structure.

The nature of lamellar, exfoliated or pseudo-tubular kaolinite was investigated by TEM (Fig. 8). The micrographs of the precursor revealed the presence of hexagonal plates, confirming that grafting did not change the morphology of the kaolinite particles. Such as previously reported [41], insertion of large polar molecules into the interlayer space could decrease the strong interaction between silica (Si–O) and aluminol (Al–OH) groups in kaolinite layers, thereby promoting the exfoliation. After complexation with the divalent cations, the structure changes, confirming the exfoliation observed by powder XRD.

Summarizing, all the catalysts have similar structures, and the complexation media can favor the exfoliation of kaolinite. Actually, the washing media control the leaching of organic moieties intercalated (non-grafted) in the kaolinite interlayer, and the amount of complexes was slighted lower in the samples washed with water.

3.2. Catalytic activity of the solids

3.2.1. Oxidation of *cis*-cyclooctene and cyclohexane

To check the activity of the catalysts prepared herein, the oxidation of the diagnostic substrate (Z)-cyclooctene by PhIO in the presence of Ka-dpa and the catalysts $\text{Me}(\text{II})\text{-(Ka-dpa)}$ at room temperature and pressure, was initially carried out (Table 1). (Z)-cyclooctene was selected as a diagnostic substrate; indeed, the high

Table 1
Yield of cyclooctenoxide (%) obtained by epoxidation of *cis*-cyclooctene with iodosylbenzene at room temperature and pressure using the indicated catalysts.

Catalyst	Time (h)			
	2	4	24	48
Mn(Ka-dpa)-IP	20	50	54	54
Ni(Ka-dpa)-IP	3	6	9	32
Co(Ka-dpa)-IP	5	10	27	31
Mn(Ka-dpa)-wt	25	50	53	62
Ni(Ka-dpa)-wt	4	8	23	29
Co(Ka-dpa)-wt	6	7	23	33
Mn(Ka-dpa)-exf	25	50	53	62
Ni(Ka-dpa)-exf	4	8	23	29
Co(Ka-dpa)-exf	6	7	23	33

Catalytic reaction conditions: 10 mg of catalyst; 0.023 mmol of PhIO ; 1.15 mmol of *cis*-cyclooctene. 1 mL of dichloroethane/acetonitrile solvent mixture.

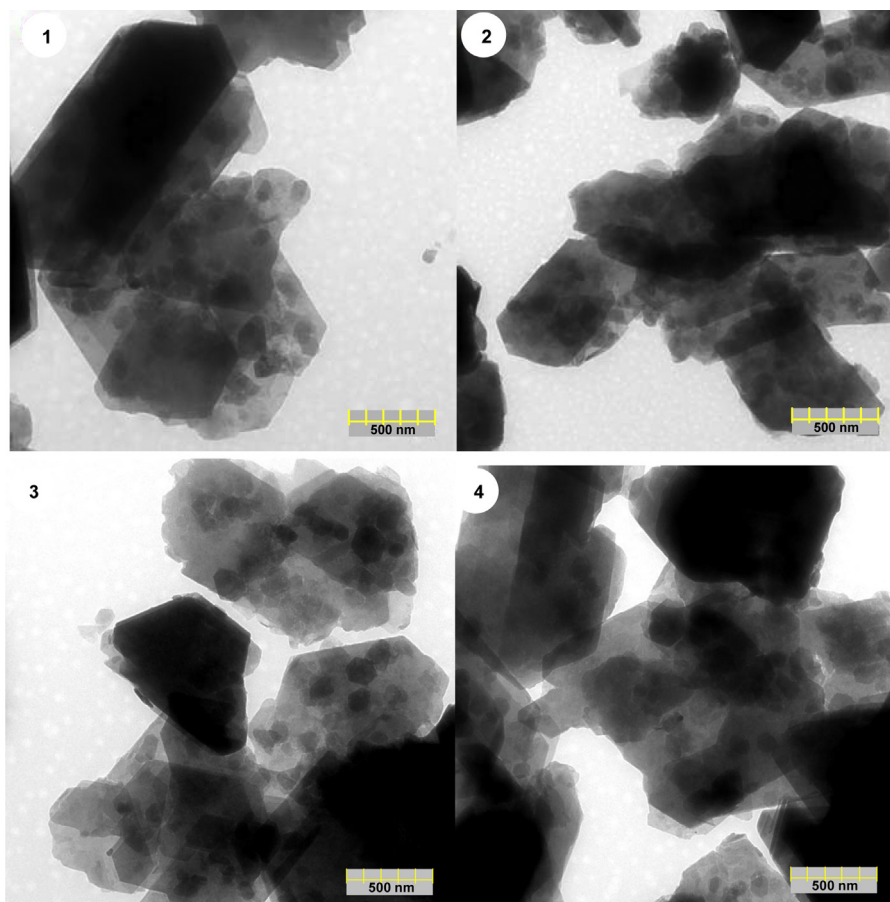


Fig. 8. TEM micrographs of the precursors (Ka-dpa)-IP (1) and Ka-dpa-wt (2), and catalysts Mn-(Ka-dpa)-IP (3) and Mn-(Ka-dpa)-wt (4).

stability of *cis*-cyclooctenoxide, its main (sometimes exclusive) oxidation product, facilitates catalyst efficiency evaluation [48]. In addition, epoxides are very useful intermediates in the chemical industry; they are the starting chemicals to prepare a wide variety of products. PhIO was used as an oxidant because of its good oxidant yields; it is relatively inert in the absence of metal complexes, generates high valent oxo-metal species and PhI, and is a polymeric solid that does not contain weak O–H bonds, thus avoiding free-radical chain reactions normally initiated by oxidants such as alkyl hydroperoxides (R–O–O–H) [49].

Control reactions were carried out in the absence of metal complexes and in the absence of oxidant (separately). These control reactions did not yield any product, not even after 48 h, although parent kaolinite contained small amounts of Fe and Ti ions.

As observed, all the Me(II)-(Ka-dpa) materials catalyzed (*Z*)-cyclooctene epoxidation by PhIO. Considering the preparation methods, Me(II)-(Ka-dpa)-IP, Me(II)-(Ka-dpa)-wt, and Me(II)-(Ka-dpa)-exf displayed a similar catalytic behavior, so these catalysts will be discussed together as Me(II)-(Ka-dpa). The selectivity to cyclooctenoxide was 100% in all cases. The epoxide yield increased along time, the best yields were achieved at 48 h of reaction. It was noted that the Mn-complex reached about 80% of their total epoxide yield at 4 h of reaction, whereas the Co- and Ni-complexes took 24 h to afford this same product yield. Furthermore, Mn(II)-(Ka-dpa) afforded a higher epoxide yield than the other catalysts. Catalytic yields decreased in the order Mn(II)-(Ka-dpa) > Co(II)-(Ka-dpa) > Ni(II)-(Ka-dpa). Two reasons account for these observations: the recognized high reactivity of the manganese cations, and the fast product diffusion from the catalyst active sites into the reaction solution [50]. It was also noted that clay exfoliation contributed

to release the product into the reaction medium; indeed, epoxide yield increased linearly with time.

It has been previously reported that when Mn-Schiff base complexes (salen or salophen) are immobilized onto a polystyrene matrix in the presence of nitrogen ligands, they are highly efficient oxidation catalysts when using single oxygen atom donors as oxidants [9,46,51]. Mirkhani et al. [51] reported that nitrogen ligands existing in the matrix act as co-catalysts, giving rise to 98% epoxide yield during (*Z*)-cyclooctene oxidation by NaIO₄ in CH₃CN/H₂O.

Although our systems afforded lower *cis*-cyclooctenoxide yield as compared to Schiff base catalysts, it may be emphasized that they offer some advantages over organic polymers, such as the high thermal and chemical stability associated to the clay. In addition, the non-toxic Mn associated to the clay is very attractive for being used in industrial processes within the principles of Green Chemistry. Reaching 100% selectivity for cyclooctenoxide is also remarkable.

The greatest issue when using transition metals as heterogeneous catalysts is to avoid catalyst leaching from the support. The UV-Vis spectra of the supernatant solutions obtained after the oxidation reactions showed that catalysts were not leached from the support in any of the studied conditions. To prove that catalysis was genuinely heterogeneous and to show the importance of adding the metal complexes to kaolinite in these reactions, the solid catalysts were filtered off the reaction mixture, extra oxidant was added to the resulting supernatant liquid, and the oxidation reaction allowed proceeding under the same initial conditions for further 48 h. After this period, *cis*-cyclooctenoxide was not detected, indicating that the catalytic activity of the materials had been really heterogeneous. However, the possibility that

Table 2
Yield of cyclooctenoxide (%) obtained by epoxidation of *cis*-cyclooctene with hydrogen peroxide at room temperature and pressure using the indicated catalysts.

Catalyst	Time (h)			
	2	4	24	48
Mn(Ka-dpa)-IP	6	12	28	55
Ni(Ka-dpa)-IP	3	8	18	35
Co(Ka-dpa)-IP	5	10	17	43
Mn(Ka-dpa)-wt	5	10	25	45
Ni(Ka-dpa)-wt	2	7	15	30
Co(Ka-dpa)-wt	4	9	16	41
Mn(Ka-dpa)-exf	5	10	25	58
Ni(Ka-dpa)-exf	4	11	20	30
Co(Ka-dpa)-exf	5	9	23	39

Catalytic reaction conditions: catalyst/H₂O₂/*cis*-cyclooctene = 1:300:100; 1 cm³ of dichloroethane/acetonitrile solvent mixture.

homogenous catalytically inactive species leached into solution cannot be ruled out.

It may be noted that the (*Z*)-cyclooctene epoxidation was not carried out under inert atmosphere, so oxygen and alkenes could have generated free radicals in the presence of the metal catalyst. To find out whether the oxidizing species originated from the reaction between the Me(II)-(Ka-dpa) materials and PhIO was different from the radical species normally detected in systems that do not involve oxo-metal species, (*Z*)-cyclooctene epoxidation was studied in the presence of hydroquinone. This radical scavenger did not diminish the product yields, so the involvement of the radical species as the epoxidizing agent can be dismissed. This fact could support the sole involvement of the active high-valent metal-oxo species in these reactions.

Catalyst reuse confirmed the high efficiency and stability of the Me(II)-(Ka-dpa) systems. The solid catalysts were separated from the reaction mixture after each experiment by simple filtration and dried before being used in a subsequent run. All the catalysts could be reused in three consecutive runs without activity loss.

It is a priority to devote attention to applying heterogeneous catalysts in combination with mild oxidants such as hydrogen peroxide [47]. This oxidant has a number of advantages: water is the only byproduct of the oxidation reactions, hydrogen peroxide shows a higher active oxygen content than other commercially available oxidants, and most of the other oxidants result from hydrogen peroxide derivatization. However, using this oxidant poses a major challenge to avoid its self-destructive disproportionation in the presence of water. Thus, to prove the efficiency of the Me(II)-(Ka-dpa) catalysts, (*Z*)-cyclooctene oxidation was carried out using hydrogen peroxide as an oxidant, and the results are included in Table 2. Again, the materials prepared by the three methods, Me(II)-(Ka-dpa)IP, Me(II)-(Ka-dpa)wt, and Me(II)-(Ka-dpa)exf, exhibited a similar behavior, so they will be discussed in general terms by referring to them as Me(II)-(Ka-dpa).

Table 2 evidences that the epoxide yield rose with time; 48 h of reaction provided the best product yields (although longer reaction times were not tested). Mn(II)-(Ka-dpa) furnished the largest alkene conversion among the catalysts here tested: Mn(II)-(Ka-dpa) > Ni(II)-(Ka-dpa) > Co(II)-(Ka-dpa). Although the manganese compound showed again the maximum efficiency, in contrast with the use of PhIO as oxidant, when hydrogen peroxide was the oxidant, the nickel complex was more efficient than the cobalt one.

No leaching of the catalysts from the matrix was detected. Therefore, catalysis was truly heterogeneous even under drastic oxidation conditions. Blank tests also confirmed that the epoxide only originated in the presence of Me(II)-(Ka-dpa). The high (*Z*)-cyclooctene conversion into the epoxide indicated that the active species during oxidation was the high valent oxo-metal species.

When the corresponding Mn-, Co- and Ni-chlorides were tested as catalysts in an homogeneous medium, the release of bubbles was observed after about five minutes of reaction, which indicated that hydrogen peroxide disproportionated occurred even before oxygen transfer from the oxidant to the substrate. Therefore, both the dipicolinic complexes present on the clay and the clay itself optimize the use of the peroxide oxidant, mimicking the site isolation principle of biological enzymes.

Castaman et al. [52] used a binuclear carboxylated bridged manganese complex immobilized on silica for epoxidation of cyclooctene by iodosylbenzene and hydrogen peroxide in homogeneous and heterogeneous media. These authors reported that Mn-complex catalysts were very efficient and selective in the epoxidation of cyclooctene by iodosylbenzene (29–74% yield of epoxide), but lower yields (1–14%) of epoxide were obtained with hydrogen peroxide. These low yields with hydrogen peroxide were attributed to the competitive parallel reaction of homolytic cleavage of hydrogen peroxide decomposition promoted by the catalysts.

Addition of the radical scavenger hydroquinone to the reaction medium did not alter the epoxide yields, dismissing the radical mechanism in our systems. Hence, only the high valent oxo-metal species were originated in the reaction medium, via oxidative heterolytic cleavage of hydrogen peroxide. This intermediate performed (*Z*)-cyclooctene oxidation and is the same active species reported for metalloporphyrins used as catalysts in epoxidation reactions with hydrogen peroxide as oxidant [53].

Berkessel et al. [54] used the Mn-salen complex to catalyze epoxidation reactions oxidized by hydrogen peroxide in the presence of imidazole, as co-catalyst. These authors reported that the peroxide underwent heterolytic cleavage, to give the metal-oxo active species. Apparently, heterolytic cleavage occurred without a co-catalyst in our system. Stamatidis et al. [55] obtained high catalytic efficiency, slightly higher than ours, when using symmetrical acetylacetonate Mn-based Schiff bases immobilized on a silica surface (by grafting and sol-gel) as catalyst for (*Z*)-cyclooctene epoxidation by hydrogen peroxide (55 vs. 70%), but their catalysts were effective and selective towards the epoxide only in the presence of ammonium acetate. Thus, our system is advantageous, because it does not require any salt or co-catalyst. Moreover, our catalysts can be reused thrice without efficiency loss (Fig. 9), while the catalysts prepared by the aforementioned authors were destroyed in the first reuse.

To confirm the efficacy and selectivity of the catalysts prepared herein, as well as the active oxidant species involved in these systems, the performance of the Me(II)-(Ka-dpa) materials as catalysts for cyclohexane oxidation was tested. Cyclohexane was chosen because it is relatively inert, has a great industrial importance and its selective oxidation into a mixture of cyclohexanol and cyclohexanone (called KA oil) is essential for the synthesis of polymers such as nylon. However, the industrial process in this case is poorly selective and carried out under drastic conditions. Therefore, the search for catalysts efficient at mild temperatures is a great challenge for both researchers and industries [56].

Table 3 shows the results obtained in the cyclohexane oxidation by PhIO catalyzed by Me(II)-(Ka-dpa) catalysts. All the Me(II)-(Ka-dpa) materials catalyzed the oxidation of the cyclohexane saturated C-H bonds, leading to 100% selectivity towards cyclohexanone. Neither cyclohexanol nor other by-products were detected.

These results highlight various aspects. First, 100% selectivity towards cyclohexanone for all the catalysts is a significant outcome. In all series the conversion rose with time; 48 h of reaction provided the best product yields. Control reactions were carried out in the absence of metal complexes and in the absence of oxidant (separately), and did not yield any products, not even at 48 h. The same reaction carried out under inert atmosphere showed a decreasing in the performance, this reduction of the yields give

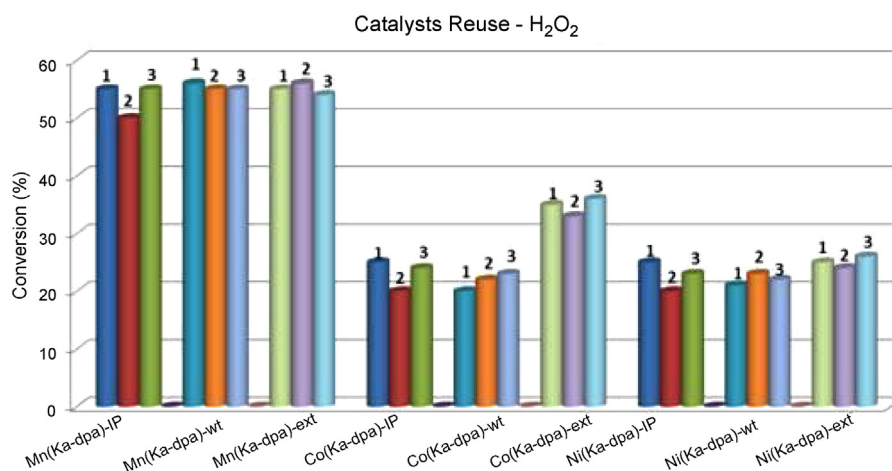


Fig. 9. Catalysts reuse of the indicated catalysts for three cycles in *cis*-cyclooctene oxidation reaction with hydrogen peroxide at room temperature and pressure.

good evidences of the possible radical mechanisms promoted by O₂ from air.

As observed in the case of (*Z*)-cyclooctene oxidation, and reported by several authors for Schiff base complex encapsulated in zeolites [9], the Mn-catalysts furnished the largest cyclohexane conversion among the metal complexes investigated here, while the activity of Co- and Ni-catalysts changes from one series to another. The catalysts were not leached from the matrix, therefore catalysis was truly heterogeneous even under the most drastic oxidation conditions used. Blank tests also confirmed that the reaction only occurred in the presence of Me(II)-(Ka-dpa). As in the case of the studies involving (*Z*)-cyclooctene as a substrate, the high selectivity towards the ketone indicated that the active species during the oxidation was the high valent oxo-metal species.

By using the Mn(III)salophen complex immobilized onto polystyrene-bound imidazole as catalyst and NaO₄ as oxidant, Mirkhani et al. [51] obtained ketone and alcohol as products, with greater selectivity for the ketone. Our material showed an advantage over this catalyst, as only the ketone was produced. Adding the radical scavenger hydroquinone to the reaction medium did not alter the ketone yields, dismissing the radical mechanism.

Hydrogen peroxide was also used to oxidize cyclohexane (Table 4). Despite lower conversion results, all the solids selectively catalyzed the oxidation of cyclohexane by hydrogen peroxide, and the ketone was the sole product. Mn(II)-(Ka-dpa) furnished the largest cyclohexane conversion among the metal complexes investigated here, Mn(II)-(Ka-dpa) > Co(II)-(Ka-dpa) > Ni(II)-(Ka-dpa). All the tests confirmed that the catalysis was truly heterogeneous and that the reaction proceeded only in the presence of the catalysts and without a radical mechanism.

Table 3

Yield of cyclohexanone (%) obtained by oxidation of cyclohexane with iodosylbenzene at room temperature and pressure using the indicated catalysts.

Catalyst	Time (h)			
	2	4	24	48
Mn(Ka-dpa)-IP	13	15	21	22
Co(Ka-dpa)-IP	0	0	12	14
Ni(Ka-dpa)-IP	0	0	13	15
Mn(Ka-dpa)-wt	13	16	22	22
Co(Ka-dpa)-wt	0	0	0	14
Ni(Ka-dpa)-wt	0	0	14	16
Mn(Ka-dpa)-exf	25	50	53	62
Co(Ka-dpa)-exf	2	4	21	25
Ni(Ka-dpa)-exf	0	3	11	17

Catalytic reaction conditions: 10 mg of catalyst; 0.023 mmol of PhIO; 1.15 mmol of cyclohexane. 1 cm³ of dichloroethane/acetonitrile solvent mixture.

Many authors have reported that by using metal complex as catalysts and hydrogen peroxide as oxidant, oxidation reactions can be improved by the addition of imidazole or sodium bicarbonate, since they act as co-catalysts and hinder hydrogen peroxide disproportionation by the metal complex (catalase-type activity) or the support [9,46,52,57]. To confirm that the homolytic mechanism did not occur in our systems, the reactions were carried out in the presence of imidazole or NaHCO₃ in the presence and absence of water. No improvement of yields or conversion was detected, confirming once more that in our systems the reaction underwent by the heterolytic cleavage of the hydrogen peroxide without involvement of the radical mechanism.

The versatile nature of the Me(II)-(Ka-dpa) catalysts in the oxidation of various substrates and oxidants tested in this work provides strong evidence that the active high valent oxo-metal species are responsible for oxygen atom transfer from the oxidant to the studied substrates, as in the case of cytochrome P450 enzymes [11].

3.2.2. Degradation of dyes

Degradation of the dyes was evaluated in terms of decolorization. Actually, total mineralization of complex molecules, such as the cationic and anionic dyes here considered, leads to the conversion of organic carbon into CO₂ and of nitrogen and sulfur heteroatoms into inorganic ions, requiring many oxidation steps and involving a large number of intermediate species. The first step of this process is usually the cleavage of the chromophoric bond, leading to the decolorization of the contaminated waters.

Results of the degradation of the three dyes considered in the present work in Fenton-like systems catalyzed by Me(II)-Ka-dpa

Table 4

Yield of cyclohexanone (%) obtained by oxidation of cyclohexane with hydrogen peroxide at room temperature and pressure using the indicated catalysts.

Catalyst	Time (h)			
	2	4	24	48
Mn(Ka-dpa)-IP	0	1	7	12
Ni(Ka-dpa)-IP	0	0	4	8
Co(Ka-dpa)-IP	0	0	4	7
Mn(Ka-dpa)-wt	0	4	10	15
Ni(Ka-dpa)-wt	0	1	8	10
Co(Ka-dpa)-wt	0	2	8	9
Mn(Ka-dpa)-exf	0	5	12	18
Ni(Ka-dpa)-exf	0	2	5	10
Co(Ka-dpa)-exf	0	3	6	13

Catalytic reaction conditions: catalyst/H₂O₂/cyclohexane = 1:300:100; 1 cm³ of dichloroethane/acetonitrile solvent mixture.

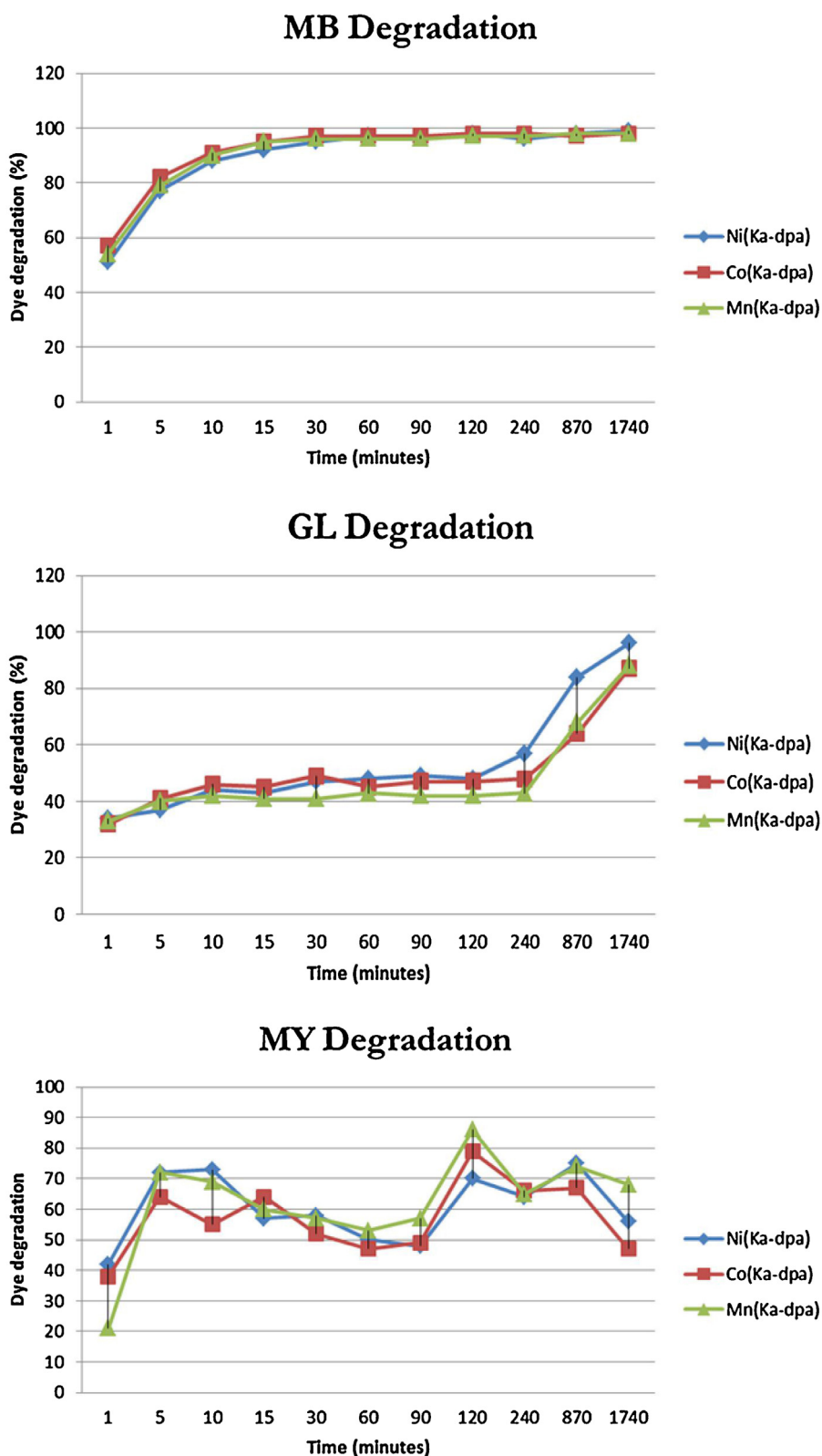


Fig. 10. Degradation of the dyes under Fenton-like conditions using the indicated catalysts.

catalysts is shown in Fig. 10 (similar results were obtained for all series, the only series washed with isopropanol is given in Fig. 10). Degradation of each of the dyes is different, as shown by the shape of the curves. In the case of MB, degradation is easy, it was higher than 80% after only 5 min of reaction, and reached 99% after 30 min. The behavior is analogous for all the catalysts. In the case of GL,

although 40% of degradation was reached after 5 min of reaction, this degradation remained practically constant, with a very small increase, up to 4 h of reaction, and a time of reaction as long as 29 h was needed to reach 90% of degradation. In this case, and for long reaction times, the Ni-catalyst showed the best efficiency. In the case of MY, the degradation reached 85% after 2 h of reaction but

decreased on extending the reaction time. This may be due to the complex structure of the dye, whose degradation may give rise to organic intermediates absorbing in close positions, a fact which can tentatively explain the non-stability with time of the degradation of MY. As previously discussed by Sleiman et al. [58], the initial steps of the reaction generally involve the hydroxylation and cleavage of –NH– bonds, resulting in the formation of benzene, aniline and phenol.

It is noticeable that the highest degradation efficiency was observed for MB, the only cationic species among the dyes studied. Although kaolinite has no cation exchange capacity, it seems that this is the dye that most efficiently interacts with the clay layers, favoring its further degradation. In summary, high decolorization (70–100%) was observed for the treated dyes at relatively short reaction times, and by means of heterogeneous processes. It is also remarkable that the reaction was completely heterogeneous, as no leaching of the catalysts was detected, which favors the reuse of the catalysts.

4. Conclusions

Kaolinites covalently grafted with dipicolinate anions proved to be suitable supports for the effective immobilization of various metal cations by forming complexes. Complexation of Ni²⁺, Co²⁺ and Mn²⁺ cations into the functionalized starting materials was efficient in all cases, leading to the formation of active heterogeneous catalysts. These catalysts were advantageous for oxidation reactions since they allowed for the use of mild conditions (room temperature and pressure, use of non-polluting oxidants) and promoted high activity and product selectivity. The catalysts were very active for *cis*-cyclooctene oxidation (about 55% yield, with total selectivity towards the epoxide), the oxidation of cyclohexane (about 22% yield, with total selectivity towards cyclohexanone), and the decolorization of dye solutions (70–100%), in this case being rather sensitive to the molecular structure of the dye. The main advantage of the kaolinite grafted complexes is their easy separation from the reaction mixture by simple filtration of the solid, thus enabling catalyst reuse.

Acknowledgments

This work has been carried out in the frame of a Spain–Brazil Interuniversity Cooperation Grant financed by MEC (PHB2011–0164–PC) and CAPES (267/12), and a Cooperation Grant from Universidad de Salamanca and FAPESP (2013/50216–0). Spanish authors thank additional financial support from Junta de Castilla y León (SA009A11–2). The Brazilian group thanks support from Brazilian Research funding agencies FAPESP (2011/17660–8 and 2012/07410–7) and CNPq, and Peróxidos do Brasil (Solvay) for kindly supplying the 70 wt.% aqueous hydrogen peroxide solution.

Appendix A. Supplementary data

Supplementary material related to this article can be found, in the online version, at <http://dx.doi.org/10.1016/j.cattod.2013.09.031>.

References

- [1] C.L. Hill, *Angew. Chem. Int. Ed.* 43 (2004) 402.
- [2] N. Bizaia, E.H. de Faria, G.P. Ricci, P.S. Calefi, E.J. Nassar, K.A.D.F. Castro, S. Nakagaki, K.J. Ciuffi, R. Trujillano, M.A. Vicente, A. Gil, S.A. Korili, *Appl. Mater. Interf.* 11 (2009) 2667.
- [3] E.H. de Faria, O.J. Lima, K.J. Ciuffi, E.J. Nassar, M.A. Vicente, R. Trujillano, P.S. Calefi, *J. Coll. Interf. Sci.* 335 (2009) 210.
- [4] E.H. de Faria, G.P. Ricci, L. Marçal, E.J. Nassar, M.A. Vicente, R. Trujillano, A. Gil, S.A. Korili, K.J. Ciuffi, P.S. Calefi, *Catal. Today* 187 (2012) 135.
- [5] A. Goti, F. Cardona, in: P. Tundo, V. Esposito (Eds.), *Green Chemical Reactions: NATO Science for Peace and Security Series C, Environmental Security*, Springer, 2008, p. 135.
- [6] V.S. Bergamaschi, IPEN-USP, Brazil (2005) (Ph.D. Thesis).
- [7] J.M. Thomas, R. Raja, *Catal. Today* 117 (2006) 31.
- [8] R. Sen, S. Bhunia, D. Mal, S. Koner, Y. Miyashita, K. Okamoto, *Langmuir* 25 (2009) 13672.
- [9] K.C. Gupta, A.K. Sutar, *Coord. Chem. Rev.* 252 (2008) 1420.
- [10] E.H. de Faria, Universidade de Franca, Brazil (2011) (Ph.D. Thesis).
- [11] M. Costas, *Coord. Chem. Rev.* 255 (2011) 2912.
- [12] K.C. Gupta, A.K. Sutar, C.-C. Lin, *Coord. Chem. Rev.* 253 (2009) 1926.
- [13] B.S. Lane, K. Burgess, *Chem. Rev.* 103 (2003) 2457.
- [14] A. Houas, H. Lachheb, M. Ksibi, E. Elaloui, C. Guillard, J.-M. Herrmann, *Appl. Catal. B* 31 (2001) 145.
- [15] M. Toor, B. Jin, *Chem. Eng. J.* 187 (2012) 79.
- [16] B. Joshi, K. Kabariya, S. Nakrani, A. Khan, F.M. Parabia, H.V. Doshi, M.C. Thakur, *Am. J. Environ. Protect.* 1 (2013) 41.
- [17] A.C. Gomes, J.C. Nunes, R.M.S. Simões, *J. Hazard. Mater.* 178 (2010) 57.
- [18] S. Papic, D. Vujevic, N. Koprivanac, D. Sinko, *J. Hazard. Mater.* 164 (2009) 1137.
- [19] Y. Tu, S. Tian, L. Kong, Y. Xiong, *Chem. Eng. J.* 185–186 (2012) 44.
- [20] E.R. Bandala, M.A. Pelaez, M.J. Salgado, L. Torres, *J. Hazard. Mater.* 151 (2008) 578.
- [21] R.L. Frost, J. Kristof, E. Horvath, J.T. Klopogge, *Spectrochim. Acta Part A* 56 (2000) 1191.
- [22] C. Detellier, J.J. Tunney, *Chem. Mater.* 5 (1993) 747.
- [23] S. Letaief, C. Detellier, *Chem. Comm.* 1 (2007) 2613.
- [24] J.G. Sharefkin, H. Saltzmann, *Org. Synth.* 43 (1963) 62.
- [25] H.J. Lucas, E.R. Kennedy, M.W. Forno, *Org. Synth.* 43 (1963) 483.
- [26] J. Murakami, T. Itagaki, K. Kuroda, *Solid State Ionics* 172 (2004) 279.
- [27] K.B. Brandt, T.A. Elbokl, C. Detellier, *J. Mater. Chem.* 13 (2003) 2566.
- [28] S. Letaief, B. Casal, P. Aranda, M.A. Martín-Luengo, E. Ruiz-Hitzky, *Appl. Clay Sci.* 22 (2003) 263.
- [29] L.R. Avila, E.H. de Faria, K.J. Ciuffi, E.J. Nassar, P.S. Calefi, M.A. Vicente, R. Trujillano, *J. Coll. Interf. Sci.* 341 (2010) 186.
- [30] E.H. de Faria, K.J. Ciuffi, E.J. Nassar, M.A. Vicente, R. Trujillano, P.S. Calefi, *Appl. Clay Sci.* 48 (2010) 516.
- [31] R.L. Frost, W.N. Martens, J. Kristof, E. Horvath, *J. Phys. Chem.* 106 (2002) 4162.
- [32] S. Letaief, C. Detellier, *Can. J. Chem.* 86 (2008) 1.
- [33] J.J. Tunney, C. Detellier, *Can. J. Chem.* 75 (2003) 1666.
- [34] M.C. MacEwan, J.L. Amoros, *Anales Edafol. Fisiol. Veg.* 9 (1950) 363.
- [35] J. Matusik, A. Gawel, E. Bielanska, K. Bahrnowski, *Clay Clay Miner.* 59 (2011) 116.
- [36] J. Matusik, E. Stodolak, K. Bahrnowski, *Appl. Clay Sci.* 51 (2011) 102.
- [37] J. Matusik, A. Gawel, E. Bielanska, W. Osuch, K. Bahrnowski, *Clay Clay Miner.* 57 (2009) 452.
- [38] N.G. Veerabadran, R.R. Price, Y.M. Lvov, *Nano Brief Rep. Rev.* 2 (2007) 115.
- [39] F. Chavarria, D.R. Paul, *Polymer* 45 (2004) 8501.
- [40] S. Nakagaki, G.S. Machado, M. Halma, A.A.S. Marangon, K.A.D.F. Castro, N. Matoso, F. Wypych, *J. Catal.* 242 (2006) 110.
- [41] J.E.F.C. Gardolinski, G. Lagaly, *Clay Miner.* 40 (2005) 547.
- [42] S. Nakagaki, F. Wypych, *J. Coll. Interf. Sci.* 315 (2007) 142.
- [43] K. Weissmerl, H.-J. Arpe, (C.R. Lindley, Trans.), *Industrial Organic Chemistry*, vol. 237, third ed., VCH Publishers, Weinheim, 1997.
- [44] M. Álvaro, B. Ferrer, H. Garcia, A. Sanjuán, *Tetrahedron* 55 (1999) 11895.
- [45] J.E. Gardolinski, F. Wypych, H.P.M. Filho, *Quim. Nova* 26 (2003) 30.
- [46] M. Tabatabaee, B.-M. Kukovec, V. Razavimahmoudabadi, *Z. Natur.* 66b (2011) 813.
- [47] J. Limburg, R.H. Crabtree, G.W. Brudvig, *Inorg. Chem.* 297 (2000) 301.
- [48] R.G. Pearson, *J. Am. Chem. Soc.* 85 (1963) 3533.
- [49] F. Gozzo, *J. Mol. Catal. A* 171 (2001) 1.
- [50] M. Salavati-Niasari, Z. Salimi, M. Bazarganipour, F. Davar, *Inorg. Chim. Acta* 362 (2009) 3715.
- [51] V. Mirkhani, M. Moghadamb, S. Tangestaninejada, B. Bahramian, *Appl. Catal. A* 311 (2006) 43.
- [52] S.T. Castaman, S. Nakagaki, R.R. Ribeiro, K.J. Ciuffi, S.M. Drechsel, *J. Mol. Catal. A* 300 (2009) 89.
- [53] T.G. Traylor, C. Kim, W.-P. Fann, C.L. Perrin, *Tetrahedron* 54 (1998) 7977.
- [54] A. Berkessel, M. Frauenkron, T. Schwenkreis, A. Steinmetz, G. Baum, D. Fenske, *J. Mol. Catal. A* 113 (1996) 321.
- [55] A. Stamatis, D. Giasafaki, K.C. Christoforidis, Y. Deligiannakis, M. Loulodi, *J. Mol. Catal. A* 319 (2010) 58.
- [56] U. Schuchardt, D. Cardoso, R. Sercheli, R. Pereira, R.S. da Cruz, M.C. Guerreiro, D. Mandelli, E.V. Spinacé, E.L. Pires, *J. Mol. Catal. A* 319 (2010) 58.
- [57] M. Ghorbanloo, H.H. Monfared, C. Janiak, *J. Mol. Catal. A* 345 (2011) 12.
- [58] M. Sleiman, D. Vildoza, C. Ferronato, J.-M. Chovelon, *Appl. Catal. B* 77 (2007) 1.